11-15 SEPTEMBER 1989

10 YEARS OF PROGRESS IN SHELL AND SPATIAL STRUCTURES

30 ANNIVERSARY OF IASS

MADRID 1989

SUMMARIES

Editors: F. del Pozo and A. de las Casas

CEDEX-LABORATORIO CENTRAL DE ESTRUCTURAS Y MATERIALES

THEME 4

NUMERICAL METHODS

THE DESIGN OF CYLINDRICAL ORTHOTROPIC PLATES AND SHELLS

by

Professor N.M. Dehousse and Dr.Ph.Rigo
Laboratoires of Hydrodynamics, Applied Hydraulics,
Hydraulic Constructions and Naval Architecture (L.H.C.N.)
University of Liège, Belgium.

SUMMARY

For 25 years ago, the field of the hydraulic structures revealed to us an extraordinary one, for which plates and shells are currently used. It is especially the case for navigation dam gates and navigation lock gates where the steel is used in relatively small thickness with a very strong stiffening.
Our studies, derived from the D.K.J. method of cylindrical shells, are presented in our paper. The method assures that the solution is always exact because the resolution principle is based on an analytic one. It is a substitute to the F.E.M. which is cumbersome to handle for the hydraulic structures.
A dedicated software (L.B.R.-3) is now available. Many designers have already been carried out with L.B.R.-3: lock gates, canal- brigdes, storm surge barrier, navigation-dam gates,...
The advantages presented by our computer programme are numerous. It is highly efficient when the stiffening is very important because it takes into account the place and the shape of the stiffeners without slowing down the resolution of the differential system. The other qualities and the advantages of the L.B.R.-3 software are quickness, simplicity, reliability, performance and its opening to every one.

THE DESIGN OF

CYLINDRICAL ORTHOTROPIC PLATES AND SHELLS

by

Professor N.M. Dehousse and Dr. Ph. RIGO

Laboratories of Hydrodynamics, Applied Hydraulics,
Hydraulic Constructions and Naval Architecture (L.H.C.N)
University of Liège, Belgium.

SUMMARY

For 25 years ago, the field of the hydraulic structures revealed to us as an extraordinary one, for which plates and shells are currently used. It is especially the case for navigation dam gates and navigation lock gates where the steel is used in relatively small thickness with a very strong stiffening.

Our studies, derived from the D.K.J. method of cylindrical shells, are presented in our paper. The method assures that the solution is always exact because the resolution principle is based on an analytic one. It is a substitute to the F.E.M. which is cumbersome to handle for the hydraulic structures.

A dedicated software (L.B.R.-3) is now available. Many designs have already been carried out with L.B.R.-3 : lock gates, canal-bridges, storm surge barrier, navigation-dam gates, ...

The advantages presented by our computer programme are numerous. It is highly efficient when the stiffening is very important because it takes into account the place and the shape of the stiffeners without slowing down the resolution of the differential system. The other qualities and the advantages of the L.B.R.-3 software are quickness, simplicity, reliability, performance and its opening to every one.

THE DESIGN OF

CYLINDRICAL ORTHOTROPIC PLATES AND SHELLS

I. INTRODUCTION

Our laboratory, the L.H.C.N. has always been interested in the hydraulic structures field. Since 25 years we have especially been dealing with the orthotropic hydraulic structures, for which plates and shells are currently used. Plates and shells with relatively small thickness and very strong stiffening are often used for navigation-dam gates, navigation-lock gates, tidal surge barriers, canal-bridges, ...

The most efficient methods for computing cylindrical orthotropic plates and shells can be grouped together under the name : *harmonic analysis methods*. The harmonic analysis method includes the finite strip, the Guyon-Massonnet method, the Golberg-Leve method, .. . All these methods are not specifically hydraulic ones. So, we propose the stiffened sheathings method, which enables us to develop the ***stiffened sheathings software, L.B.R.-3*** (Logiciel des Bordages Raidis- version 3).

II. THE DEVELOPMENT OF THE STIFFENED SHEATHINGS SOFTWARE L.B.R.-3.

Our studies, derived from the D.K.J. method of cylindrical shells (Donnell, von-Karman, Jenkins), evolved as follows :

FIRST STEP

- *Setting up a system of three differential equations for thin plates and shells without stiffening.*

The basic equations were the Flugge ones. We were interested by the concrete shell roof design.

- *Study of concrete shell roofs prestressed by curved cables.*

- *Setting up of a system of three differential equations for orthotropic plates and shells with an uneven stiffening.*

To solve this last system easily, the Fourier series have to be used. Usually it is supposed that the stiffeners (longitudinal and transversal) are evenly distributed. In fact, the hydrostatic loading excludes the use of an equal spacing for the longitudinal (horizontal) direction.

For the cross-bars, which are not evenly distributed, we solved this system by the Volterra-Fredholm integral equations and by using the Green functions associated to the three differential equations.

SECOND STEP

- *computation of simple rectangular orthotropic plane sheathings simply-supported along two vertical lines.*

We recall that with the Fourier series, the end conditions are w=Mx=0 (displacement and bending moment). Then the plates are always considered as simply-supported along two vertical lines; the two horizontal supports can be fixed, free, supported, ...

A lock-gate with a simple sheathings and 3 cross-bars was the first important application of our method.

- *computation of box gates using many orthotropic plane elements*

This new step allows the design of a double-sheathings gate, for exemple : a maritime lock-gate .

THIRD STEP

- *computation of box gates using plates and shells, both of them orthotropic with simple supports along two vertical lines.*
- *computation of box gates using orthotropic plates and shells with any boundary conditions along vertical lines.*

III. THEORETICAL STATEMENTS

The basic element is a cylindrical shell where the length is L and the radius q. The coordinates system is presented in figure 1, the axis OX along the cylindrical generator, the axis Oφ along the circonference and OZ perpendicularly to the shell. Displacements u,v and w are associated to the OX, Oφ and OZ axis.

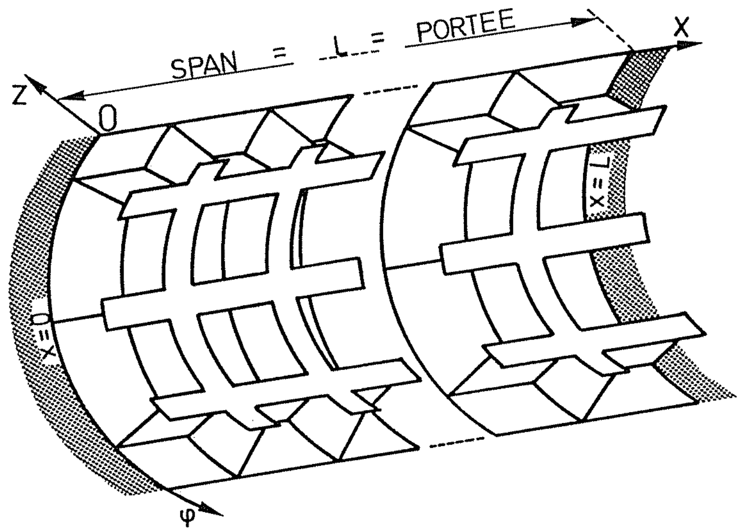

FIGURE 1: Cylindrical shell element .

III.1. The D.K.J. equations.

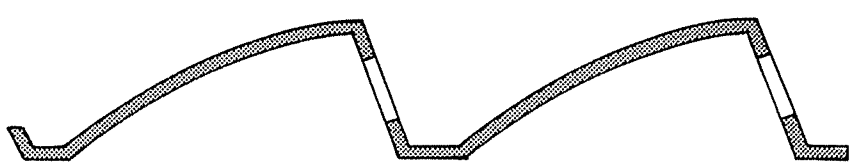

FIGURE 2 : Concrete shell shed roof.

Starting from the 3 differential equations of the thin plates and shells without stiffening, we have established coefficient tables which allow us to design shell. The application field is the design of concrete shell roof as sheds (fig. 2).

III.2. Prestressed concrete shell.

The load can be dead load or hydrostatic pressure but also specific pressure as X,Y and Z which are oriented respectively along the 3 axis OX, Oφ and OZ. By using adequate combinations of X,Y and Z loads, it is possible to compute shells which are prestressed by curved cables.

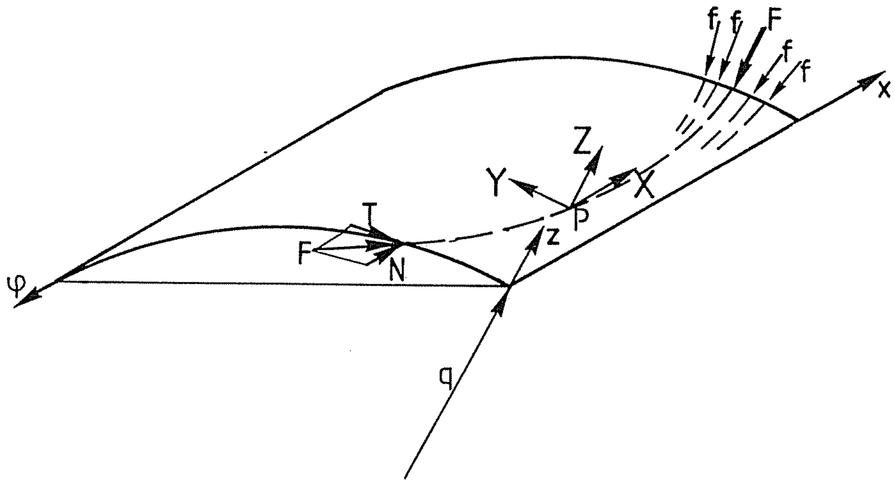

FIGURE 3 : Concrete shell roof with curved prestressed cables..

III.3. The differential equations of stiffened shells.

The basic element is now a cylindrical orthotropic shell (fig. 4).

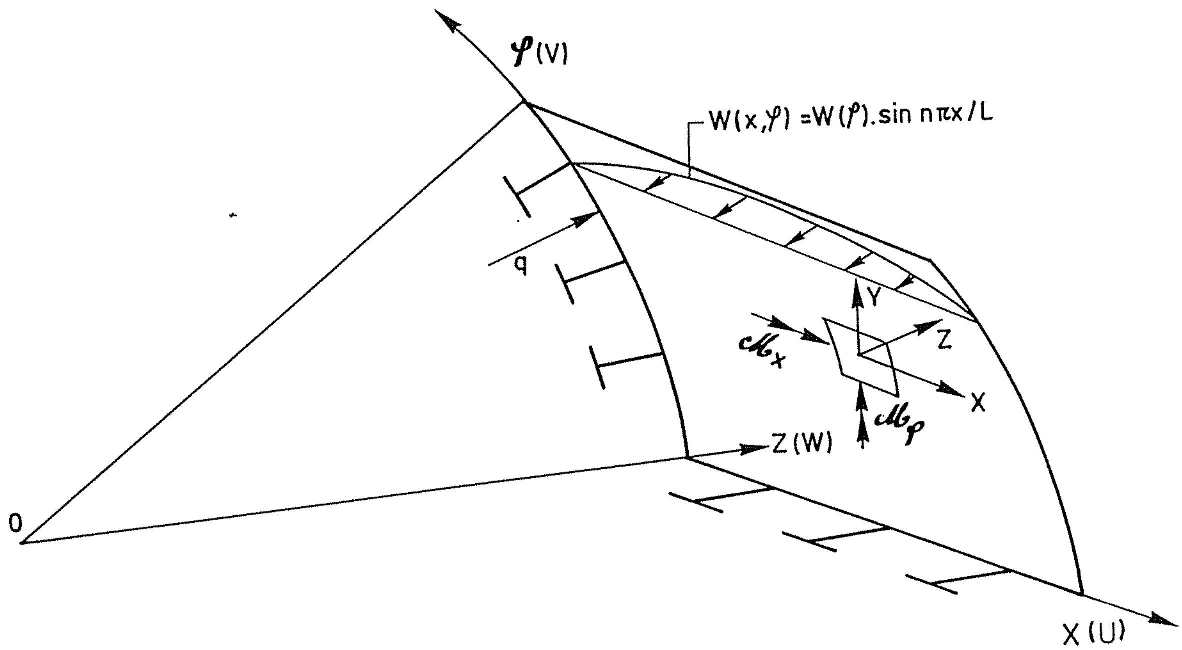

FIGURE 4 : Shell element with longitudinal and transversal stiffeners.

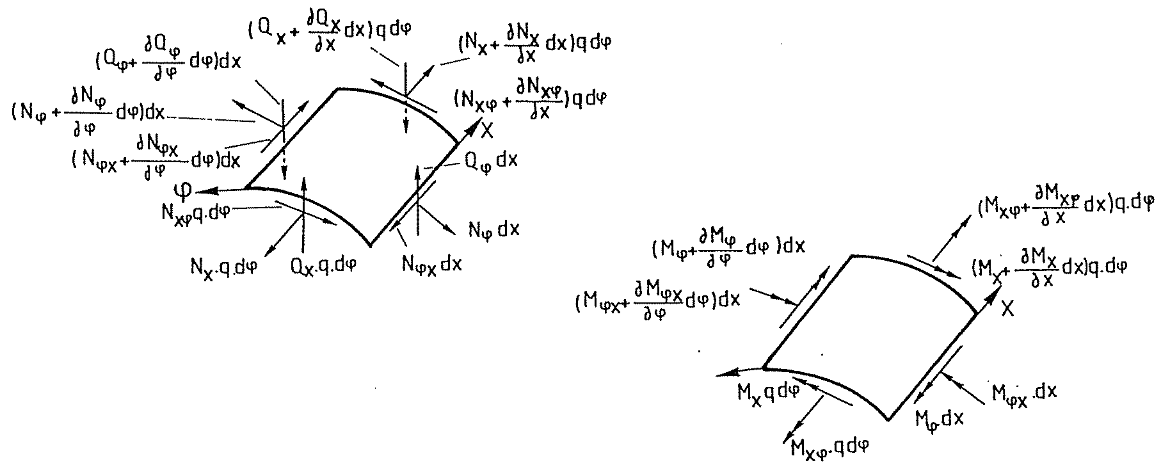

FIGURE 5 : Unitary forces and moments.

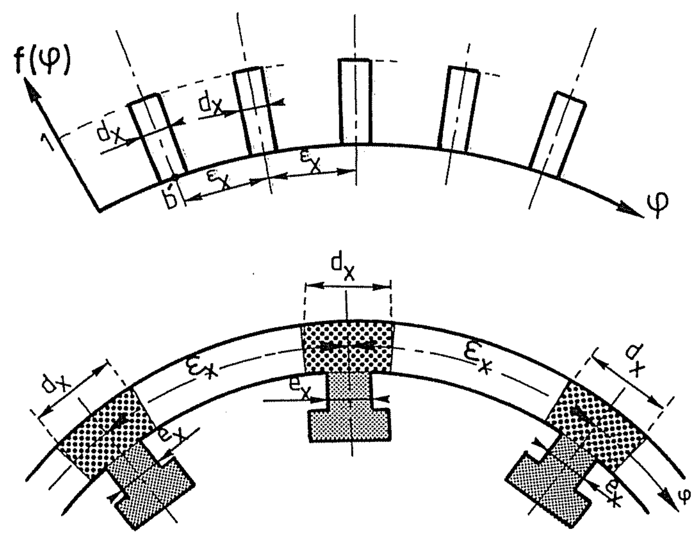

FIGURE 6 : Diagram of the f(φ) functions which allow us to take exactly into account the place of the different types of stiffeners.

This reference shell includes 3 types of stiffening ribs (longitudinal and transversal stiffeners, cross-bars). These longitudinal and transversal ribs have respectively a spacing of ε_x and ε_φ. There are also the forces (N_x, N_φ, $N_{x\varphi}$, $N_{\varphi x}$, Q_x, Q_φ) and the moments (M_x, M_φ, $M_{x\varphi}$ et $M_{\varphi x}$) which are computed with respect to the mean surface (fig. 5).

The f(φ) function are composed by Heaviside ones. These enable to obtain (fig. 6) functions perfectly compatible with the structural geometry. They are egal to the unity but cancel out the spaces (d_x et d_φ) where the ribs act.

So, we determine the 6 equilibrium equations containing the 10 aforementioned unknown variables (fig. 5).

$$N'_x + N^\circ_{\varphi x} /q + X + g_x \, \delta = 0 \qquad (1)$$

$$N^\circ_\varphi /q + N'_{x\varphi} - Q_\varphi /q + Y + g_\varphi \delta = 0 \tag{2}$$

$$N_\varphi/q + Q^\circ_\varphi /q + Q'_x = Z + g_z \delta \tag{3}$$

$$M^\circ_\varphi /q + M'_{x\varphi} - Q_\varphi + \mathcal{M}_x = 0 \tag{4}$$

$$M'_x + M^\circ_{\varphi x} /q - Q_x - \mathcal{M}_\varphi = 0 \tag{5}$$

$$N_{x\varphi} - N_{\varphi x} + M_{\varphi x}/q + \mathcal{M}_z = 0 \tag{6}$$

with $df/dx = f'$ and $df/d\varphi = f^\circ$

To write the expression of the forces and moments (figure 6) in function of the u,v and w displacements, the two constants D and K which are dependant of the material (E Young modulus, ν Poisson coefficient) and δ the shell thickness, we proceed in the following way :

It must be borne in mind the equilibrium of an infinitesimal element in only two dimensions. The third one is neglected, we considere only the mean surface.

In order to write the equilibrium of this element, we introduce forces like for instance

$$N_x = \int_{-\frac{\delta}{2}}^{+\frac{\delta}{2}} \sigma_x \left(1 + \frac{z}{q}\right) dz \tag{7}$$

Taking into account of the stress-deformations relationships, we obtain for an unstiffened shell,

$$N_x = D/q \,.\, (u'\, q + \nu v^\circ + \nu w) \qquad \text{avec } D = E\, \delta/(1-\nu^2) \tag{8}$$

With longitudinal stiffeners, the expression (7) is not any more valid and has to be changed to:

$$N_x = \int_{-\frac{\delta}{2}}^{+\frac{\delta}{2}} \sigma_x \left(1 + \frac{z}{q}\right) dz \; + f(\varphi) \int_{\omega_x} \sigma_x \frac{e_x}{d_x} dz \tag{9}$$

with e_x the stiffeners' width
d_x the maximal width where the stiffeners act
ω_x the stiffener cross-section
$f(\varphi)$ the Heaviside function which is 1 under the stiffeners and 0 otherwise (fig. 6).

After integration of the (9) relationship, we have :

$$N_x = D/q \,.\, (u'\, q + \nu v^\circ + \nu w) + f(\varphi)\ (E/d_x).(u'\, \omega_x - w''\, h_x) \tag{10}$$

with h_x the static moment with respect to the mean surface.

We obtain again $N_{x\varphi}$.

$$N_{x\varphi} = D(1-\nu)/2 \,.\, (v' + u^{\circ}/q) + f(\varphi)\ (G/d_x).\ \Omega'_x \,.\, (v' + u^{\circ}/q) \qquad (11)$$

Following the same procedure we will obtain $N_{x\varphi}$ M_x et $M_{x\varphi}$,N_{φ}, $N_{\varphi x}$ M_{φ} et $M_{\varphi x}$.

Concerning the Q_x et Q_{φ} relationships, they are determined from the (4) and (5) moment equations by introducing the already computed forces and moments.

After, replacing the forces and moments by their analytical expressions in the three equations (1) to (3), we obtain a system of three differential equations with constant coefficients, (12) to (14). This system, about the stiffened cylindrical shell are only function of the u,v and w displacements and their derivatives.

$$\begin{aligned} & D\,(q\,u''+\nu\, v^{\circ\prime}+\nu\, w') + D/q^2\,.(1-\nu)/2\,.\,(u^{\circ\circ}+q\, v^{\circ\prime}) + f(x).[S_{\varphi}/q\ (v^{\circ\prime} + u^{\circ\circ}/q)\,] \\ & \quad + f^{\circ}(\varphi)/q\ [\,S_x\ (v' + u^{\circ}/q)\,] + f(\varphi)\ [\Omega_x\, u'' - H_x\, w''' + S_x/q\,.\,(v^{\circ\prime} + u^{\circ\circ}/q)\,] + X = 0 \qquad (12) \end{aligned}$$

$$\begin{aligned} & D/q^2\,(v^{\circ\circ} + w^{\circ} + \nu\, q\, u^{\circ\prime}) + D/q\,.(1-\nu)/2\,.\,(u^{\circ\prime}+q\, v'') \\ & \quad + f(x).[\Omega_{\varphi}/q^2\,.\,(v^{\circ\circ} + w^{\circ}) - H_{\varphi}/q^3\,.\,w^{\circ\circ\circ} + S_{\varphi}\,(v'' + u^{\circ\prime}/q)\,] \\ & \quad + f'(x)/q\ [\,S_{\varphi}\ (v' + u^{\circ}/q)\,] + f(\varphi)\ [\,S_x\ (v'' + u^{\circ\prime}/q)\,]\ + Y = 0 \qquad (13) \end{aligned}$$

$$\begin{aligned} & D/q^2\,(v^{\circ} + w + \nu\, q\, u') + K/q^4\,.\,w^{\circ\circ\circ\circ} + 2.K/q^2\,.\,w^{\circ\circ\prime\prime} + K\, w'''' \\ & \quad + f(x)\ [\ \Omega_{\varphi}/q^2\,.\,(v^{\circ} + w) - 2\,H_{\varphi}/q^3\,.\,w^{\circ\circ} - \\ & \qquad\quad H_{\varphi}/q^3\,.\,v^{\circ\circ\circ} + R_{\varphi}/q^4\,.\,w^{\circ\circ\circ\circ} + T_{\varphi}/q^2\,.\,w^{\circ\circ\prime\prime} + L_{\varphi}/q\ .\,(v^{\circ\prime\prime} + u^{\circ\circ\prime})\,] \\ & \quad + f(\varphi)\ [\ T_x/q^2\,.\,w^{\circ\circ\prime\prime} + L_x/q\,.\,(v^{\circ\prime\prime} + u^{\circ\circ\prime}/q) - H_x\,.\,u''' + R_x\,.\,w''''\,] \\ & \quad + f^{\circ}(\varphi)/q\ [\ T_x/q\,.\,w^{\circ\prime\prime} + L_x/q\,.\,(v'' + u^{\circ\prime}/q)\,] \\ & \quad + f'(x)\ [\ T_{\varphi}/q\,.\,w^{\circ\prime\prime} + L_{\varphi}/q\,.\,(v'' + u^{\circ\prime}/q)\,] = -\,\mathcal{M}^{\circ}{}_x/q + \mathcal{M}'_{\varphi} + Z \qquad (14) \end{aligned}$$

where $\Omega_x,H_x,T_x,L_x,S_x,R_x$ are parameters depending upon the longitudinal stiffeners geometry,

$\Omega_{\varphi},H_{\varphi},T_{\varphi},L_{\varphi},S_{\varphi},R_{\varphi}$ are parameters depending upon the transversal stiffeners geometry,

After reduction, we come to one 8th order differential equation of w with two variables, x and φ.

$$A.\, w^{\prime\prime\prime\prime\,\prime\prime\prime\prime} + B.w^{\prime\prime\prime\prime\,\prime\prime} + C.w^{\prime\prime\prime\prime\,\prime\prime\circ\circ} + D.w^{\prime\prime\prime\prime} + E.w^{\prime\prime\prime\prime\,\circ\circ} + F.w^{\prime\prime\prime\prime\,\circ\circ\circ\circ} + G.w^{\prime\prime\circ\circ} + I.\, w^{\circ\circ\circ\circ\,\prime\prime} + J.w^{\circ\circ\circ\circ\,\prime\prime\circ\circ} + K.w^{\circ\circ\circ\circ\,\circ\circ\circ\circ} = 0 \quad (15)$$

with $w^{\circ} = dw/d\varphi$, $w' = dw/dx$, $w'^{\circ} = d^2w\,/\,dx.d\varphi$, ...

The A,B,C, ...,J et K coefficients are constants, depending upon the geometrical characteristics of the shell and its stiffeners, and also of the physical properties of the material (E,ν).

To obtain an equation which two separated variables, we develop the displacements according to the Fourier series system.

$$w(x,\varphi) = \sum_{n=1}^{\infty} w(\varphi)\ \sin(n\pi x/L) \qquad (16)$$

$$v(x,\varphi) = \sum_{n=1}^{\infty} v(\varphi)\ \sin(n\pi x/L) \qquad (17)$$

$$u(x,\varphi) = \sum_{n=1}^{\infty} u(\varphi)\ \cos(n\pi x/L) \qquad (18)$$

III.4. The simply supported plates.

For a good understanding, it is necessary to recall the end conditions of a simply supported structure.

The sine-serie developments of $w(x,\varphi)$ (16), has fixed the other displacement expressions : $v(x,\varphi)$ as $\sin\lambda x$ (17) and $u(x,\varphi)$ as $\cos\lambda x$ (18). So, at the ends ($x=0$ and $x=L$), the displacements w and v are zero but the longitudinal displacement u is not zero.

If the both ends ($x=0$ and $x=L$) are always simply supported, the two other ones ($\varphi=0$ and $\varphi=\varphi_0$) can be free, simply supported, fixed, ...

The first version of the stiffened sheathings software was efficient for the stiffened plates. It allowed us to compute a lifting lock-gate (fig.7).

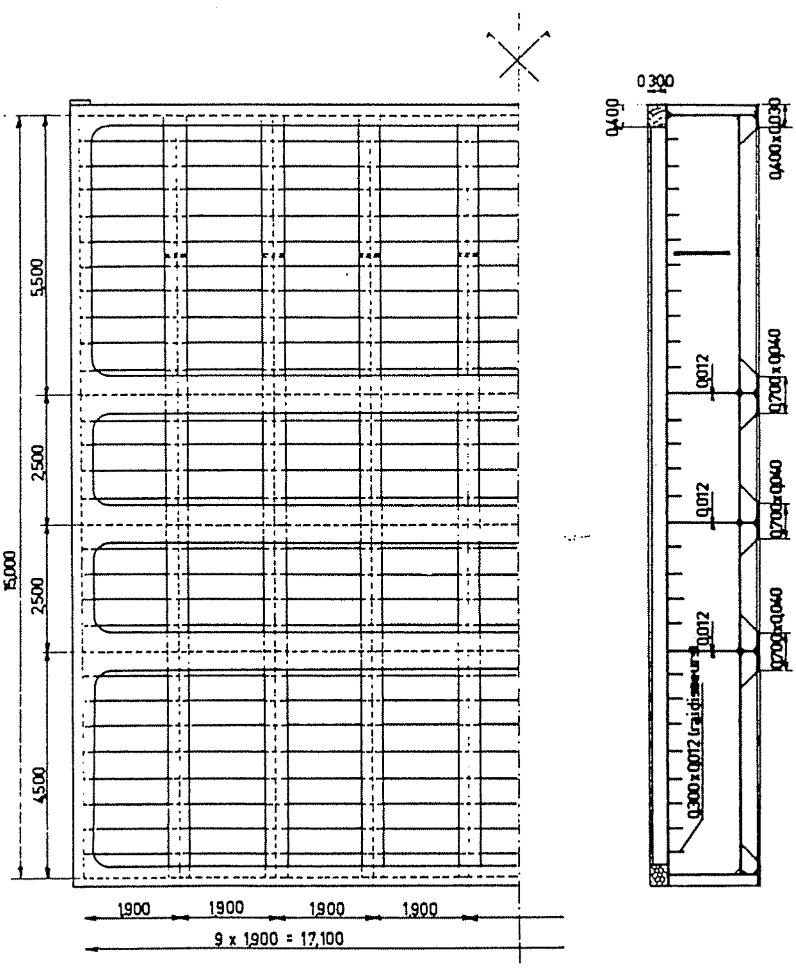

FIGURE 7 : Simple sheathing lock gate

III.5. Simply supported box-structures.

The box-structures are composed of many plate or shell elements. At the junction along OX between two elements, the end conditions are four continuity equations and four equilibrium equations. For example, at the junction figure 8, we have :

$$w_1 = v_2, \ldots, u_1 = u_2, \ldots$$

and

$$(N_\varphi)_1 + (Q_\varphi)_2 = 0$$
$$(M_\varphi)_1 + (M_\varphi)_2 = 0$$
$$(Q_\varphi)_1 + (N_\varphi)_2 = 0$$
$$(N_{x\varphi})_1 + (N_{x\varphi})_2 = 0$$

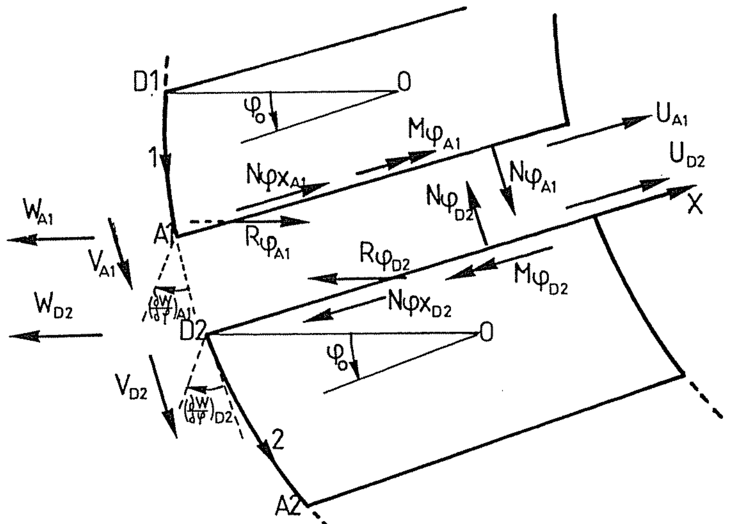

FIGURE 8 : Junction between two shells.

For example, with this new type of conditions, we can compute a maritime lock gate (fig. 9).

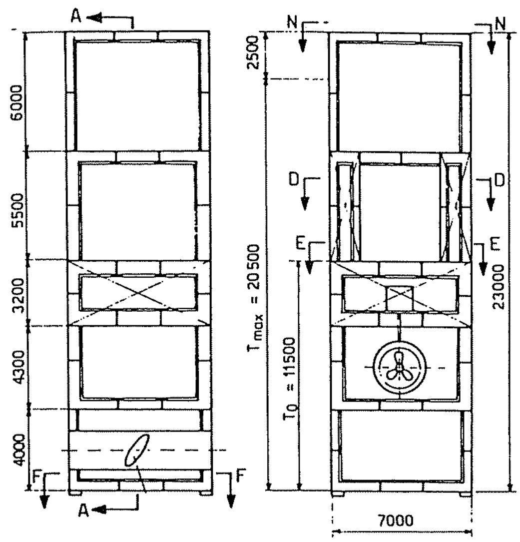

FIGURE 9 : A maritime lock gate.

III.6 The Fourier series applied to structures with particular end conditions.

In the last version of the stiffened sheathings software, special external forces are included such as classic external forces X,Y and Z. Among these external forces, there are also ***end-forces*** N_b and ***end-moments*** M_b which are applied at both ends of the plates and the shells of the structures (figure 10). These end-forces and end-moments enable us to simulate, for exemple, the forces and the moments that the supporting arms of a radial gate transmit to the box-girder (fig. 11).

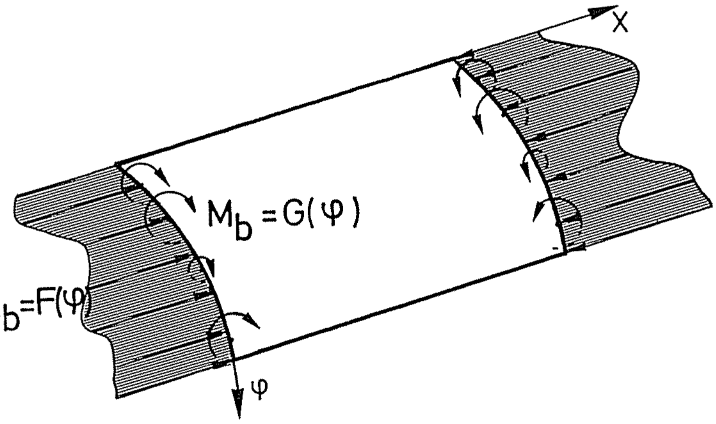

FIGURE 10 : End forces N_b and end moments M_b.

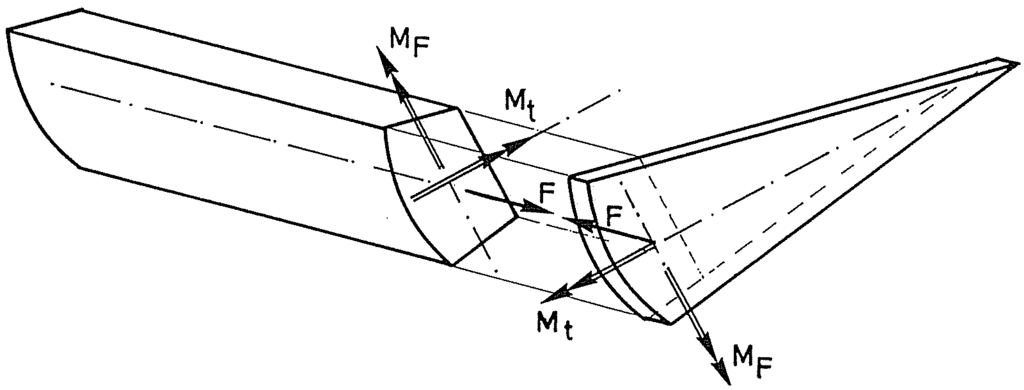

FIGURE 11 : Forces and moments at the junction between the box-girder and a supporting arm.

Concerning the end forces, we use the development of two end loads F. The analytical expression of the end forces N_b is :

$$N_b = \sum_{n=1}^{\infty} \left[{}^{4}/(2n-1)\pi d^* . F . (-1)^{n+1} . \cos[(2n-1)\pi(L-2d^*)/L] . \cos[(2n-1)\pi x/L] \right] \qquad (19)$$

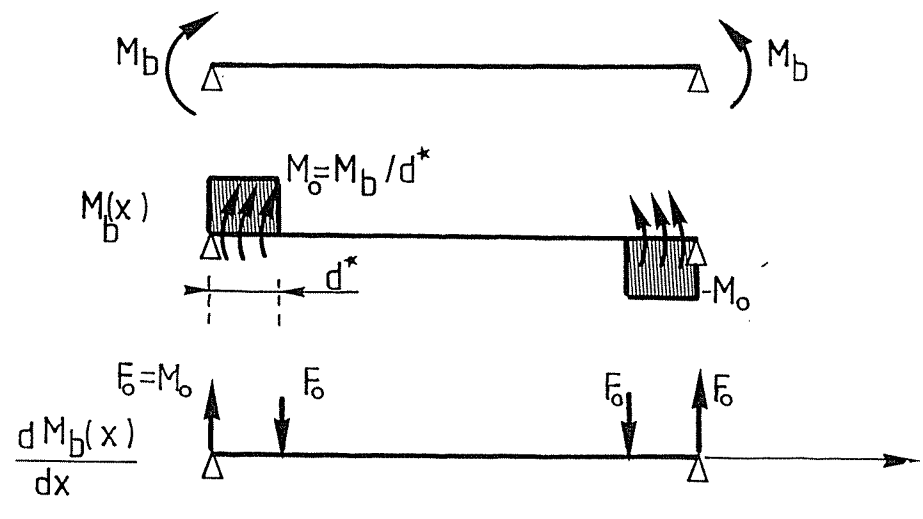

FIGURE 12 : End moments M_b.

For the end moments, we use the same method. However, there is an important difference, only the derivative of the external load $\mathcal{M}_{\varphi}$ exists in the differential equations (12, 13 and 14). So, we must consider the derivative of the end moments M_b (fig. 12).

The development of this end moment M_b (20) according to the Fourier series is the following one :

$$M_b(x) = \sum_{n=1}^{\infty} \left[4\, M_b / (2n-1)\pi d^* \, . \, (-1)^{n+1} \, . \, \cos[(2n-1)\pi(L-2d^*)/L] \, . \, \cos[(2n-1)\pi x/L] \right] \qquad (20)$$

$$dM_b/dx = \sum_{n=1}^{\infty} \left[4/(2n-1)\pi d^* \, . H \, . \, (-1)^{n+1} \, . \, \cos[(2n-1)\pi(L-2d^*)/L] \, . \, \sin[(2n-1)\pi x/L] \right] \qquad (21)$$

$$H = -(2n-1)\pi/L \, . \, M_b$$

The end force N_b and the moment derivative $\mathbf{dM_b/dx}$ have the same analytical expression. In the first expression (19), F is the applied force which is constant for all the terms of the Fourier series. In the expression (21), H has the dimension of a force, but it varies with every term. It is a function of the end moment M_b.

III.6.1. Fourier series development of the end forces and end moments.

The figure 13 shows that the end moments development requires an important number of terms, especially if we must get an exact load representation. Indeed, for the current applications, 7 terms are enough to have a sufficient accuracy.

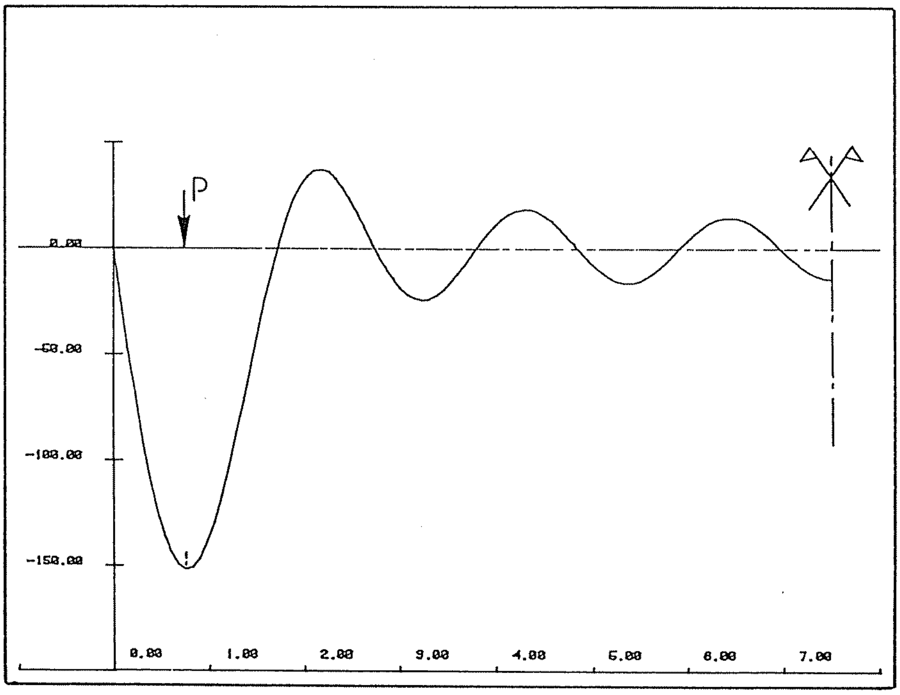

FIGURE 13 : Diagram of a concentrated load with 7 terms of the Fourier series.

In practice, concentrated loads do not exist. They are always more or less spread on small lengths near the ends. So, the end forces N_b and the end moments M_b are applied on small lengths near the ends and we obtain successful results with only 7 terms of the Fourier series (fig. 14)

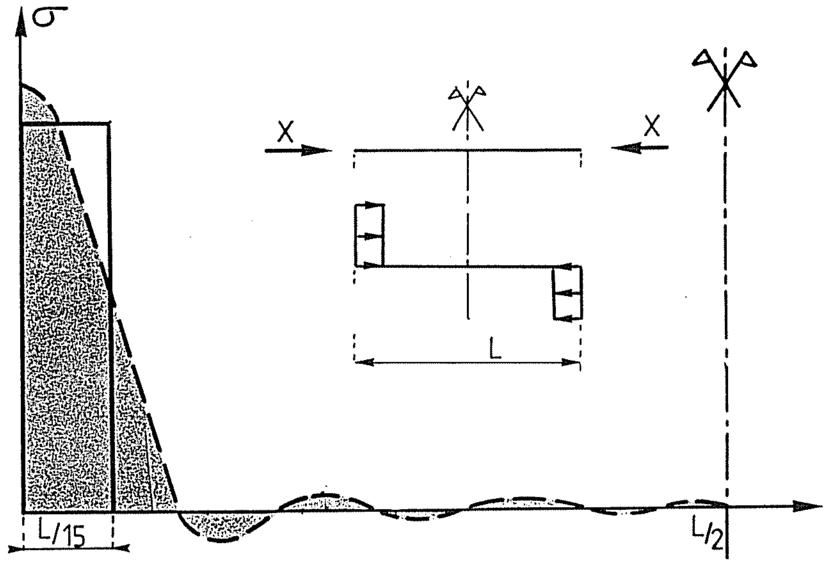

FIGURE 14 : Development of a load which is applied on the ends over small lenghts d*=L/15.

IV. FIELD UTILIZATION OF THE END FORCES AND MOMENTS.

The figure 15 shows the end deformations of a box-girder. These are the u displacements and the dw/dx rotations at each shell ends.

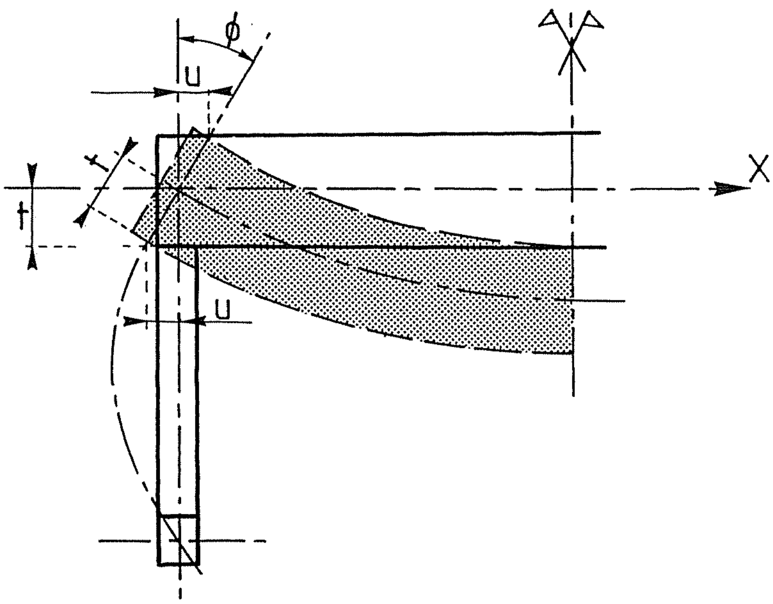

FIGURE 15 : End deformation of a box-girder.

We can analyze the case of an elastically supported box-girder. For example, the box-girder and the supporting arms of a radial gate behave like a portal (fig. 16). The end sections of the gate cannot have any such deformation as it is possible for a simply supported gate.

If the end of a supporting arm is submitted to a general rotation ϕ, the longitudinal displacements u and the rotations dw/dx at the junction *box-girder/arm* are automatically known as function of this variable ϕ. It is necessary to apply at the ends, end forces N_b and end moments M_b which must together lead to coincidence between the end displacements of the box-girder and those ones resulting from the arm rotation.

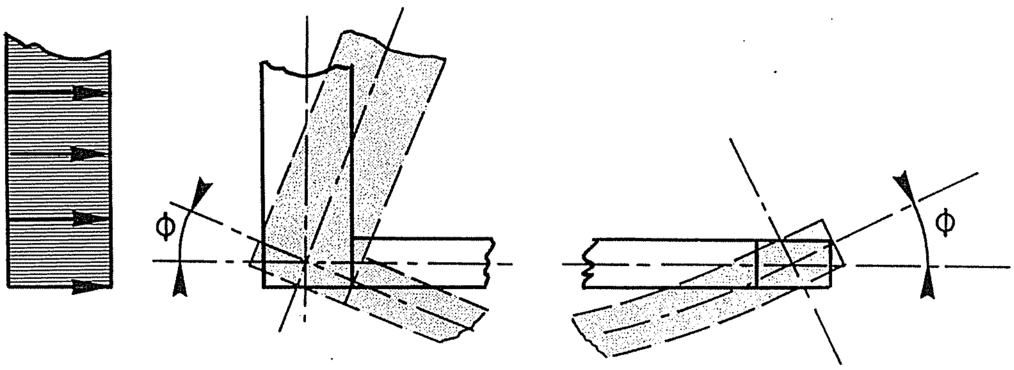

FIGURE 16 : Plan of the portal, the box-girder and a supporting arm of a radial gate.

How to proceed in practice ?

Consider figure 17, a structure loaded by a hydraulic pressure (hydrostatic and hydrodynamic pressures). The moment Mbr (fig. 17) applied at the junctions *box-girder/arm* is important if the relative arms stiffness next to the box-girder increases.

At the junction *box-girder/arm*, we have to realize the compatibility of the displacement u and the rotations dw/dx. Then, we split the behaviour of the portal into two parts, the arm one and the box-girder one. So, we analyze the two parts separately.

Concerning the arms, we have a relationship between the moment M_{br} , applied at the supporting arm ends and the rotation ϕ (fig. 17).

On the other hand, for the box-girder, we can determine the end forces and the end moments associated to displacements and rotations which are the same of the arms ones. Let Mv be the resulting moment of the end effects (forces and moments).

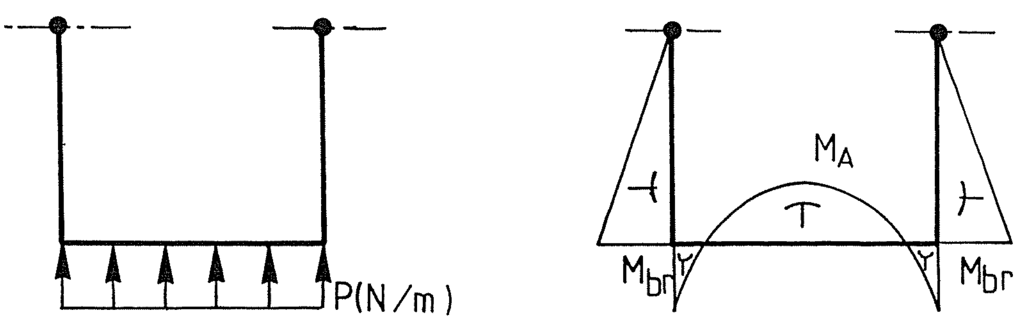

FIGURE 17 : Moment diagram in the portal structure (*box-girder/arms*).

After that, we have to adjust the Mbr moment of the arm with the Mv moment of the box-girder (fig. 18).

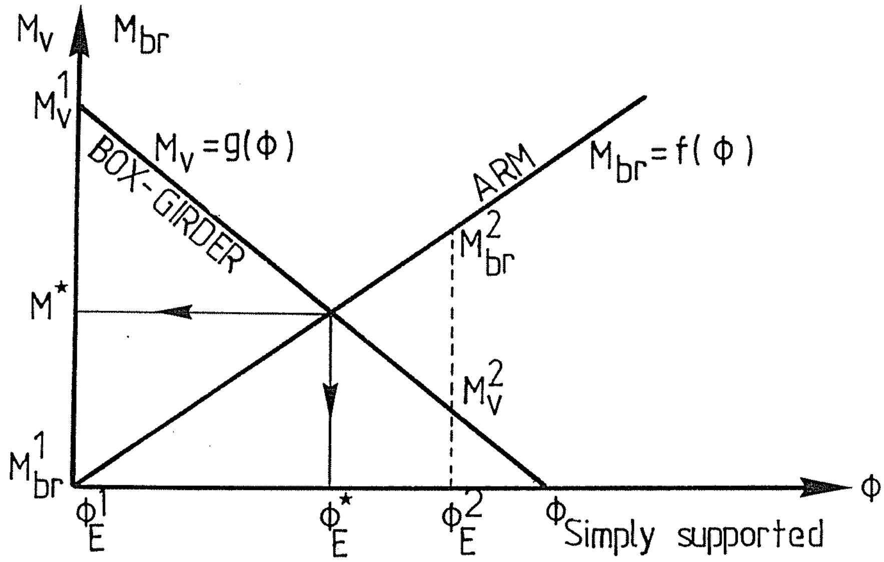

FIGURE 18 : Diagram of the M_V and M_{br} moments in function of the ϕ rotation at the junction *box-girder/arms*.

V. HYDRAULIC STRUCTURES APPLICATIONS.

Radial gate (fig. 19), sector gate (fig. 20), flap gate (fig. 21) and lifting gate (fig. 22) are four examples of navigation-dam gates. Today, the structural engineer designs the navigation-dams with very long spans. Therefore, he uses frequently box-girders which are stiffened by longitudinal and transversal stiffeners.

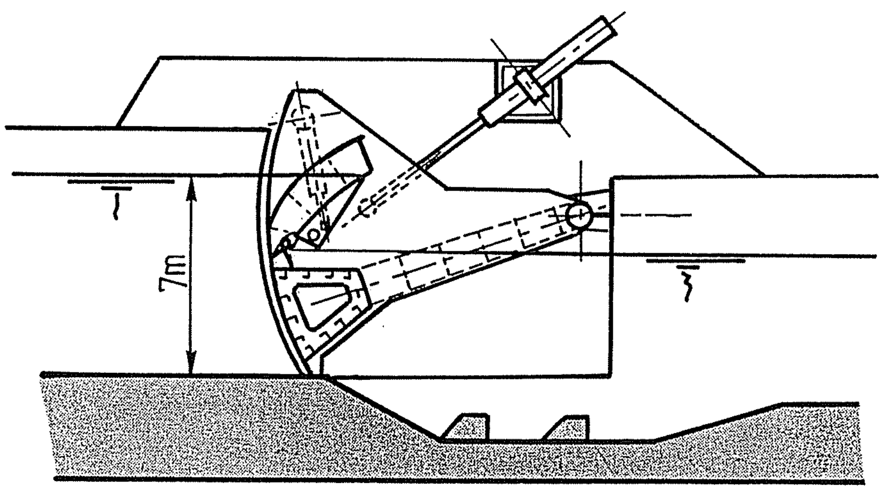

FIGURE 19 : Radial gate

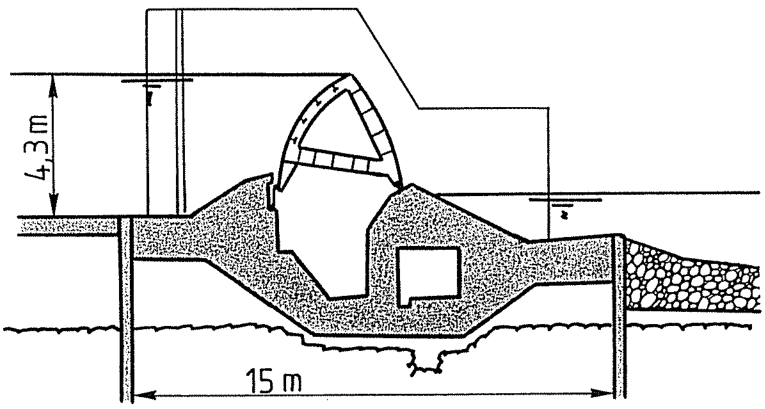

FIGURE 20 : Sector gate

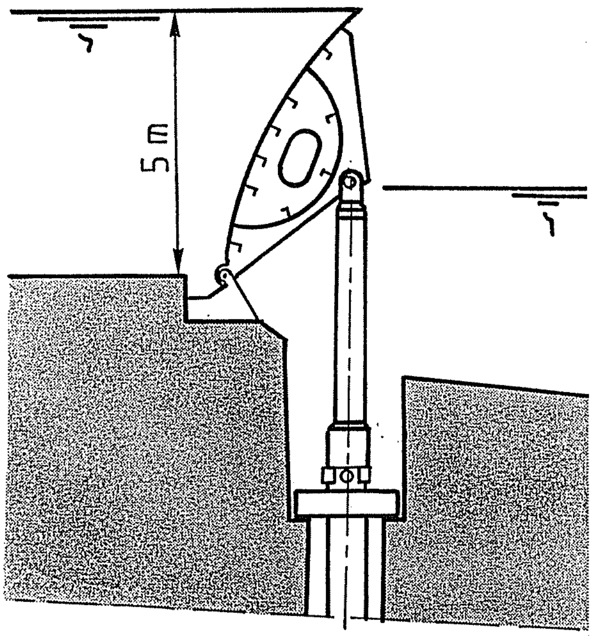

FIGURE 21 : Flap gate

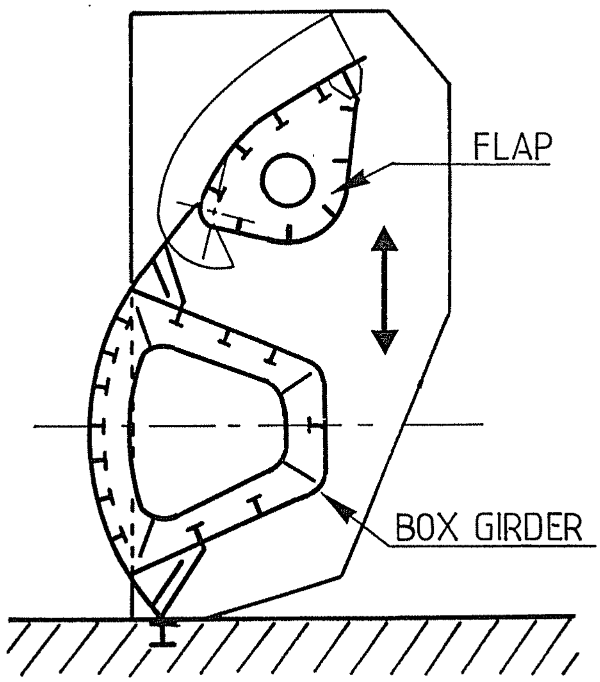

FIGURE 22 : Lifting gate.

The same procedure is used for a lock-gate or a canal-bridge. For such structures, the number of the stiffeners and cross-bars is so important that treating them by F.E.M. becomes very expensive. Indeed, the computing time for a simple sheathing lock-gate needs 90 minutes CPU on an IBM 3081 (réf. 9). So, for such structures, the F.E.M. is cumbersome to handle and a more appropriate method is highly necessary. As alternative of the F.E.M., we propose the L.B.R.-3 utilization.

With the design and the computation of a navigation-dam gate, we will show as concisely as possible the L.B.R.-3 software qualities.

V.1. The radial gate of a navigation-dam.

As we explained in the introduction, the main piece of modern navigation-dam gates is nowadays an open or closed box-girder which is composed of plates and shells. This main piece can very easily be computed by our L.B.R.-3 software.

We have chosen to present the case of a radial gate (fig. 23) for which the study is particulary delicate and for which the geometrical caracteristics are noted below.

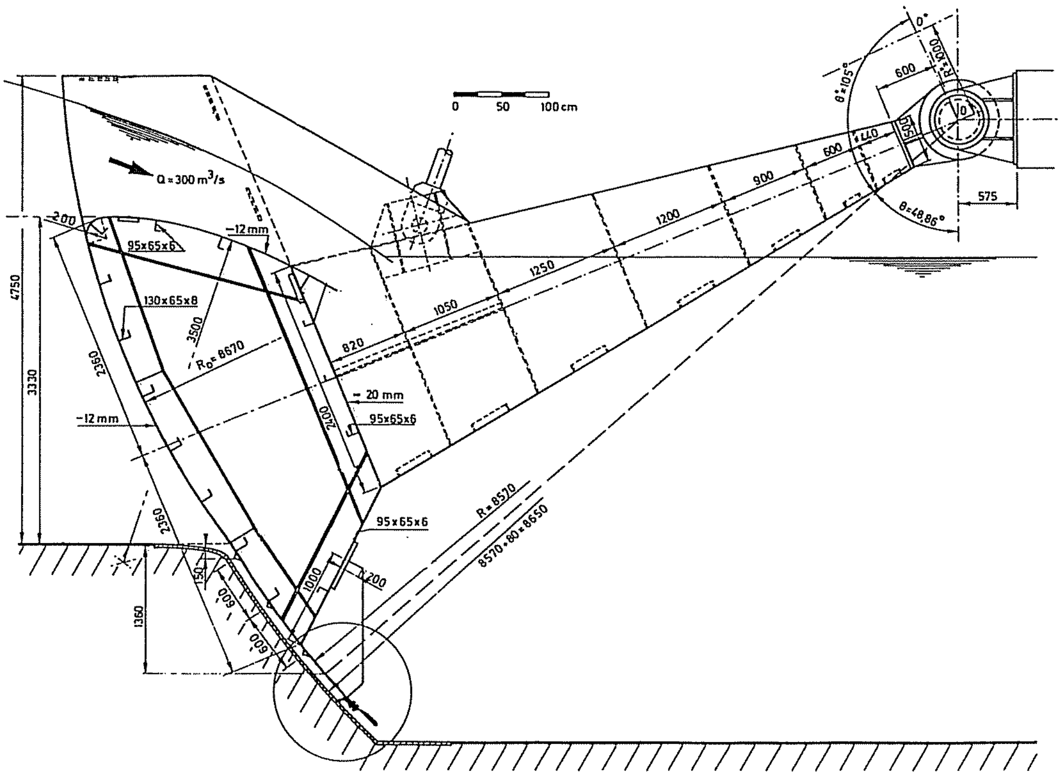

FIGURE 23 : Cross-section of the radial gate.

Upstream panel :	longitudinal stiffeners	:	300x150x10	(0.6m spaced)
	transversal stiffeners	:	130x65x8	(1.8m spaced)
Up and down panels :	longitudinal stiffeners	:	300x150x10	(0.6m spaced)
	transversal stiffeners	:	95x65x6	(1.8m spaced)
Downstream panel :	longitudinal stiffeners	:	300x150x10	(0.6m spaced)
	transversal stiffeners	:	95x65x6	(1.8m spaced)

The first computation carried out with the L.B.R.-3 software has enabled us to control the pilot-study. These computations carried out with 1 term and without the end effects (gate supposed simply-supported) demands only 72 data lines and 20 s. CPU on an IBM 4381. The last checkings realized with 7 terms and the end forces Nb and the end moments Mb require 3 more data lines and 7 min. CPU.

The extremely reduced data and the very short computation time (CPU) confirm the interest for the designer to use the L.B.R.-3 software in order to design such a structure. Moreover, L.B.R.-3 provides a varied range of numerous, reliable results. So, the complete computing of a complex structure like this radial gate, can be accomplished within 8 hours (discretization, data correction, computing, printing and results analysis). This very short computation time represents a great importance for a designer, because, this way, he can get a quick confirmation of the good or the bad behaviour of his projected structure.

Owing to the characteristics previously mentioned, we can obtain the diagrams of the displacements, the stresses and the forces acting in the structure. So, the figure 24 shows the transversal stresses σ_φ diagram in the sheathing at mid-span.

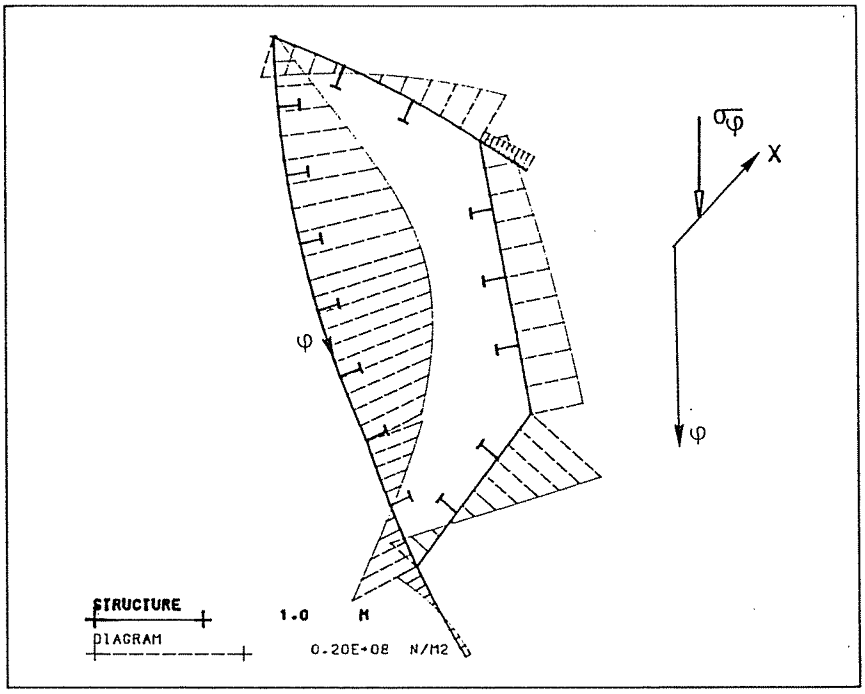

FIGURE 24 : Transversal stresses σ_φ diagram in the sheathing at mid-span (x=L/2).

VI. CONCLUSION.

Our studies evolved following 3 steps. The first step was a theorical one and it concerned the thin shells which can be prestressed by curved cables. The second one corresponded to the beginning of the computer study of a simply supported box structure.

The third one includes also an important theorical part concerning an original extension of the D.K.J. method. Indeed, we can now compute with the Fourier series any structure with any boundary conditions. Moreover, it contains all the computer development about the shells. These developments enabled us to estabish an efficient tool : the L.B.R.-3 software.

To increase the application field of our method, we have added to the classic external forces N_b, end forces and end moments M_b. These last ones are applied at both ends of the shells.

L.B.R.-3 enables us to compute very complex structures, such as navigation-dam gate, tidal surge barrier, lock gate, canal bridge. The complete computing of a such complex structures can be accomplished within a few hours (discretization, data correction, computing, printing and results analysis).

The main advantages and qualities of the L.B.R.-3 software are : quickness, simplicity, reliability, performance, ... However the most important one is surely its "accessibility". Indeed, using L.B.R.-3 only demands a short training and a little competence, it is at every one's level.

VII. BIBLIOGRAPHY

1. N. M. DEHOUSSE, "Les couvertures en voile mince de forme cylindrique et de section circulaire", Bulletin du CERES, tome VII, Liège, Belgium, 1955.

2. N. M. DEHOUSSE, Discussion at 2d Symposium on Concrete Shell Roof Construction, Teknish Ukeblad Oslo, Norway 1957.

3. J. E. GOLBERG, H. L. LEVE, "Theory of Prismatic Folded Plate Structures", Mémoires AIPC, Vol 17, Zurich, Zwitzerland, 1957.

4. N. M. DEHOUSSE, " Les bordages raidis en construction hydraulique", Mémoires du CERES (Nouvelle série), Vol. n°1, Liège, Belgium, 1961.

5. R. BARES, Ch. MASSONNET, "Le calcul des grillages de poutres et dalles orthotropes", DUNOD, Paris, France, 1966.

6. N. M. DEHOUSSE, J. DEPREZ, "Les bordages orthotropes plans, Calcul d'une porte d'écluse", Mémoires du CERES (Nouvelle série), Vol n°22, Liège, Belgium, 1967.

7. Y. K. CHEUNG, "Finite Strip Method Analysis of Elastic Slabs", Journal of the Engineering Mechanics Division, ASCE, Vol 94, n°EM6, USA, 1968.

8. Ph. BEGUIN,"Calcul et optimalisation de portes d'écluses de grandes dimensions à double bordage", Faculté des Sciences Appliquées, Université de Liège, Belgium, 1982.

9. P. ARISTAGHES, P. LEBRETON, F. VANSTEENKISTE, "Calcul des portes d'écluses maritimes", AIPCN, bulletin n°52, Brussels, Belgium, 1986.

10. L.H.C.H., "Stormvloedkering, Nieuwe Waterweg", Rapport interne du LHCN de l'Université de Liège, Belgium, 1987.

11. Ph. RIGO, "Applications des développements harmoniques aux calculs des ouvrages hydrauliques métalliques", Collection des Publications de la Faculté des Sciences Appliquées de l'Université de Liège, Belgium, 1989.